Proceedings of the 3rd IASME/WSEAS Int. Conf. on FLUID DYNAMICS & AERODYNAMICS, Corfu, Greece, August 20-22, 2005 (pp267-272)

# 2D and 3D Computation for Two Phase Flow by Large Eddy Simulation and a Lagrangian Model

K.F. YU[1], K.S. LAU[1], C.K. CHAN[2], H.Q. ZHANG[3]
[1] Department of Applied Physics, [2] Department of Applied Mathematics,
The Hong Kong Polytechnic University, Hung Hom, Hong Kong, CHINA
[3] Department of Engineering Mechanics. Tsinghua University, Beijing, CHINA
kf.yu@polyu.edu.hk

*Abstract:* - In simulations of many engineering problems, such as mixing layer flow, channel flow and jet flow etc., it is common to assume the turbulent flows as two-dimensional in order to reduce computation time. Turbulence is however a three-dimensional phenomenon. Simulation in two dimensions may lose a lot of information such as the more realistic vortex structures. In this paper, 2D and 3D simulation results are compared by calculating a two-phase turbulent flow over a backward-facing step. In the simulation, the gas phase is performed by Large Eddy Simulation and the particle phase is traced by a Lagrangian tracking model. The simulation is carried out with the flow parameters and geometry of the test section similar to those of the experiment performed by Fessler and Eaton [1]. Reynolds number of the gas phase over the backward facing step with an expansion ratio of 5:3 is 18,400, based on the maximum inlet velocity and step height. In this paper, the flow is considered as dilute. Hence a one way coupling method is applied, in which we only consider the effect of fluid on the particle. Particle-particle collisions are also neglected. Both 2D and 3D predicted statistical mean properties such as mean velocity profile, fluctuating velocity profile and reattachment length of both phases are compared with experimental results. Instantaneous turbulent flow structure simulated in 2D and 3D are also compared. 2D and 3D Particle dispersions are further numerically investigated by introducing into the backward facing step sphere particles with different Stokes numbers.

*Key-Words:* - Large eddy simulation; Backward-facing step; Two-phase; Turbulent

## 1 Introduction

Two-phase flows occur frequently in many engineering and natural processes. A typical application to natural processes involves predicting of pollutants dispersion in our living environment. Hunt [2] has gave a review on environmental particulate problem. Engineering application of two-phase flow includes pulverized-coal combustion, spray combustion and solid transport. A detailed discussion of such two-phase flow problem can be found in Sirignano [3] and Ghosh and Hunt [4]. Describing and predicting the turbulent characteristics of two-phase flows is therefore an important research topic in applied fluid mechanics. Flow in many engineering devices often includes flow separation and flow reattachment. Momentum exchange in the region of flow separation and reattachment vary greatly. It may have significant effect on the performance of devices such as heat exchangers and combustion units. Backward-facing step, which provides structures of both flow separation and reattachment, is used frequently in many experimental and numerical studies.

Several numerical calculations have been carried out on backward-facing step flows, assuming two-dimensional flow with either single phase [5, 6] or two-phase [7, 8] simulation. Three dimensional simulations have also been carried out by some researchers in single phase [9] and two-phase laminar flows [10]. Two-dimensional simulation has the advantage of requiring less computational time and less memory compared with three-dimensional simulation. However, turbulence is essentially a three-dimensional phenomenon. Two-dimensional simulation may lose a lot of information of the three-dimensional vortex structures. In this paper, 2D and 3D simulation results are compared by calculating a two-phase turbulent flow over a backward-facing step. In the simulation, the gas phase is performed by Large Eddy Simulation and the particle phase is traced using a Lagrangian tracking model.

## 2 Configuration

Figure 1 shows the 3D schematic diagram of the simulation geometry, based on the experiment setup by Fessler and Eaton [1]. The backward-facing step has an expansion ratio of 5:3. Reynolds number of the air flow over the backward-facing step is 18,400, based on the maximum inlet velocity ($U$) of 10.5

$ms^{-1}$ and step height (*H*) 26.7 mm. Particles introduced into the flow are glass spheres of density 2,500 $kgm^{-3}$ and different diameters with. Both 2D 3D simulation are performed and compared in the present study.

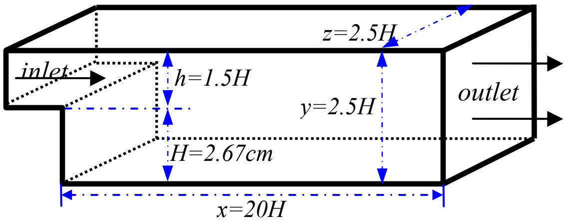


Fig. 1 Schematic diagram of the simulation geometry

## 3 Equations for fluid phase

Large eddy simulation (LES) is used to simulate the gas phase of the flow. The flow field variables are separated into a large-scale component and a subgrid scale (SGS) component by filtering. The effect of the subgrid scales on the resolved scales is modelled by the SGS stress according to the Smagorinsky [11] model. The space filtered time dependent incompressible Navier-Stokes equations with Smagorinsky model in Cartesian coordinates can then be written as

$$\frac{\partial \rho u_j}{\partial x_j} = 0 , \qquad (1)$$

$$\frac{\partial \rho u_i}{\partial t} + \frac{\partial \rho u_i u_j}{\partial x_j} = -\frac{\partial p}{\partial x_i} + \frac{\partial}{\partial x_j}\left[\mu^*\left(\frac{\partial u_i}{\partial x_j} + \frac{\partial u_j}{\partial x_i}\right)\right] , \qquad (2)$$

where $i$ = 1, 2, 3 refers to the $x$ (streamwise), $y$ (transverse) and $z$ (spanwise) directions respectively for 3D and $i$ = 1, 2 for 2D simulation. $\mu^* = \mu + \mu_T$, where $\mu$ is the dynamic viscosity and $\mu_T$ is the eddy viscosity given by $\mu_T = \rho(C_S\Delta)^2\sqrt{2S_{ij}S_{ij}}$ . $S_{ij}$ is the rate of strain tensor of the filtered velocity field, $\Delta = \sqrt{\Delta x \cdot \Delta y \cdot \Delta z}$ is the filter width. After careful numerical experiments, $Cs$ = 0.048 and $Cs$ = 0.17 are chosen as the Smagorinsky model parameter for 2D and 3D simulation respectively. The equations have been nondimensionalized, using the step height as the length scale, the maximum inlet velocity as the velocity scale and the ratio of step height and maximum inlet velocity as the time scale.

The governing equations are discretized spatially on a staggered Cartesian grid. The flow was resolved using 259 x 34 x 34 grid points in the $x$, $y$, and $z$ directions for 3D simulation and 259 x 34 grid points for 2D simulation. Derivatives are approximated using central difference for the diffusion terms while the advection terms are discretized by a skew-symmetric form [12]. Time integration of the governing equations is carried out with a third-order Runge-Kutta method. The time step is taken as 0.005 in both 2D and 3D simulation. Chorin's fractional-step projection method [13] is adopted in solving the incompressible gas-phase equations. The Poisson equation for pressure correction is formed and solved directly using Fourier series expansion in the streamwise and spanwise directions with tri-diagonal matrix inversion [14].

The inlet velocity condition of the simulation is set as the mean velocity profile of channel flow with velocity fluctuation generated from a cosine function [15]. The maximum amplitude of the fluctuation velocity is limited at 10% of the inlet velocity. No slip boundary condition for velocity is applied at the top and bottom solid walls where the pressure gradient is set as zero. Periodicity boundary condition is assumed in the spanwise direction in the 3D simulation. In order to prevent waves reflecting from the outlet, a convective open boundary condition [16] is applied at the outlet.

## 4 Equations for particle phase

Flow field of the particles is simulated and visualized when the fluid phase has become steady. 200 particles are evenly spaced along the inlet and added at intervals of 10 time-steps. There are totally 600,000 particles introduced into the backward facing step at the end of the simulation. Lagrangian approach is employed to predict the properties of each particle directly from the equations of motion. The other assumptions for the particle motion are

1. All particles are rigid spheres with equal diameter and density.
2. The density of the particles is assumed large compared with that of the fluid.
3. Particle-particle interactions are negligible.
4. Dilute two-phase particle-laden flow is assumed and effect of the particles on the flow structures is neglected.
5. Collisions with boundaries are assumed to be elastic.

The governing equations for a particle along its trajectory with drag and gravitational forces can be written as

$$\frac{d\vec{x}_p}{dt} = \vec{u}_p , \qquad (3)$$

$$\frac{d\vec{u}_p}{dt} = \frac{\vec{f}^{drag}}{m_p} + \vec{g} , \qquad (4)$$

where $\bar{u}_p$ is the instantaneous particle velocity, $\bar{x}_p$ is the displacement of particle, $m_p$ is the mass of particle, $\bar{f}^{drag}$ is the drag force and $\bar{g}$ is the gravitational acceleration. The drag and gravitational force of a single particle in a uniform flow field can be generally expressed by [17]

$$\bar{f}^{drag} = C_d \frac{1}{4}\pi d_p^2 \frac{\rho_f}{2}\left|\bar{u}_f - \bar{u}_p\right|\left(\bar{u}_f - \bar{u}_p\right), \tag{5}$$

where $d_p$ is the diameter of the particle, $\rho_f$ and $\bar{u}_f$ are the density and velocity of the fluid respectively, $\bar{g}$ is the gravitation acceleration and $C_d$ is the drag coefficients [18] given by

$$\begin{aligned} C_d &= \frac{24}{Re_p}(1+0.15Re_p^{0.687}) \quad ; \quad Re_p \le 1000, \\ C_d &= 0.44 \quad ; \quad Re_p > 1000, \end{aligned} \tag{6}$$

The particle Reynolds number, $Re_p$ is defined by

$$Re_p = \frac{\rho_f \left|\bar{u}_f - \bar{u}_p\right| d_p}{\mu_f}. \tag{7}$$

Where $\mu_f$ is the fluid viscosity.

## 4 Results and discussions

### 4.1 Statistical velocity profile for fluid phase

Figure 2 and Fig. 3 show the predicted 2D and 3D mean streamline flow pattern respectively. The predicted reattachment lengths of 7.41H in 2D simulation and 8.0H in 3D simulation agree well with the experimental value of 7.4H. The 2D simulation result is closer to the experimental result.

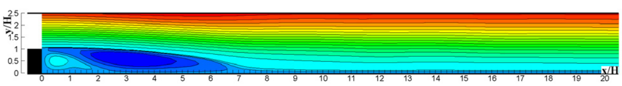

Fig. 2. Mean 2D streamline (gas)

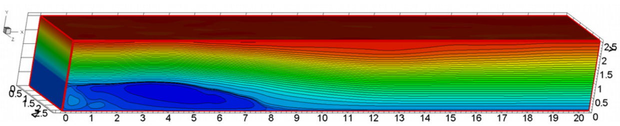

Fig. 3. Mean 3D streamline (gas)

Both 2D and 3D predicted mean velocity profiles of the gas phase are in good agreement with experimental results of Fessler and Eaton [1] at different downstream position of $x/H$ = 2, 5, 7, 9 and 14 as shown in Fig. 4.

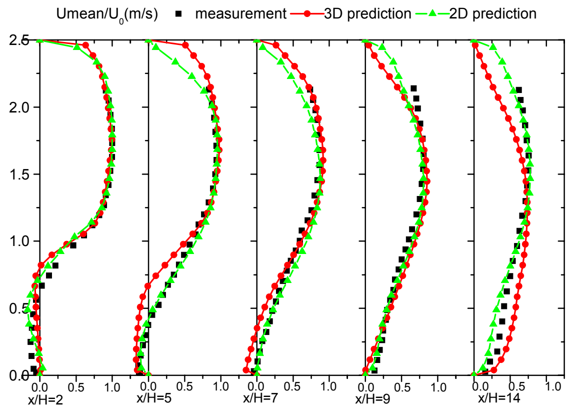


Fig. 4. Streamwise mean velocity (gas)

3D predicted fluctuating properties such as streamwise and transverse fluctuating velocity profiles of the gas phase are also in good agreement with experimental results as shown in Fig. 5-6, but there is large discrepancy between 2D predicted fluctuating properties and experimental results as shown in Fig. 5-6. The 2D predicted results are higher than experimental results, especially near the top and bottom wall regions. The 2D computation has serious limitation in predicting fluctuation properties of the turbulent flow. In other words, 2D computation can only reveal the properties of mean flow, but not fluctuating properties of turbulence of the gas phase.

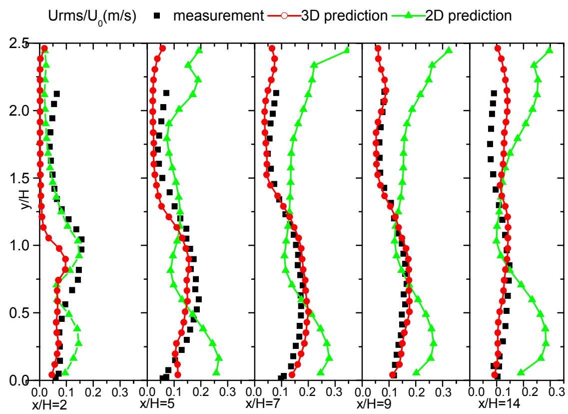


Fig. 5. Streamwise fluctuating velocity (gas)

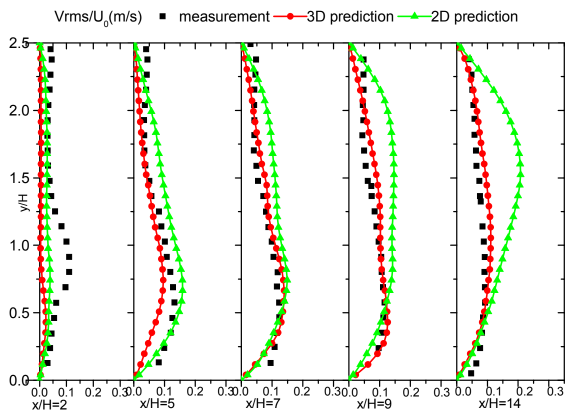


Fig. 6. Transverse fluctuating velocity (gas)

There are still large discrepancy between 3D simulation results and experimental value for section $x/H = 2$. In the present paper, the inlet velocity condition of simulation is set as the mean velocity profile of channel flow with velocity fluctuation generated from a cosine function [15]. This fluctuation may not reproduce the turbulence at the inlet and may have no correlations in space and time. However, a fully developed turbulent flow can be self-established for down stream.

## 4.2 Statistical velocity profiles for particle phase

In the numerical simulation, 150µm glass particles with initial velocities of 92% of those of the fluid phase are introduced to the backward-facing step according to the experimental finding [1]. The predicted result of particle phase is similar as the gas phase. Both the 2D and 3D predicted mean velocity profiles of particle phases are in good agreement with experimental results at different downstream position $x/H = 2$, 5, 7, 9 and 14 as shown in Fig. 7.

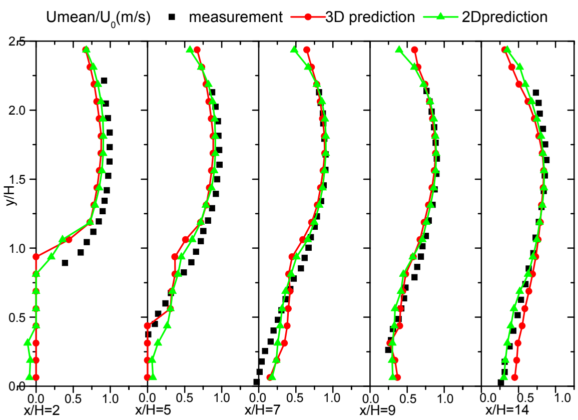


Fig. 7. Streamwise mean velocity (particle)

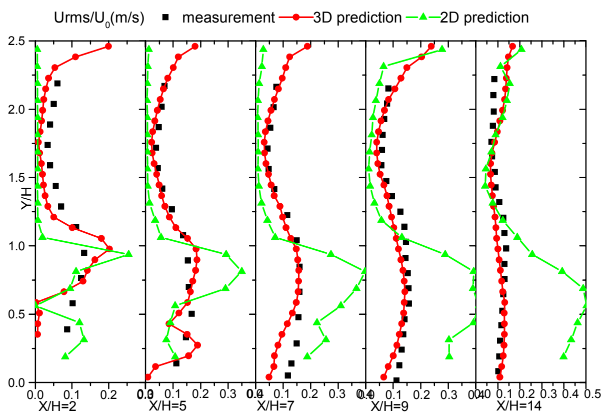


Fig. 8. Streamwise fluctuating velocity (particle)

However, there is large discrepancy for the streamwise fluctuating velocity of 150µm glass particle between 2D results and experimental results, while 3D results are in good agreement as shown in Fig. 8. So 2D computation can only reveal the properties of the mean flow, but not the fluctuating properties of turbulence of particle phase. Discrepancy occurs in 3D prediction for lower part of sections at $x/H = 2$ and 5 as shown in Fig. 8. According to the simulation result, only a few 150µm glass particles with Stokes number of 7.3 are found in the recirculation zone. The phenomena is consistent with the results of Hardalupas et al [19], who found that only particles with Stokes number less than 1 can be dispersed into the recirculation zone. This may lead to statistical error caused by the scarcity of particles in the zone.

## 4.3 Instantaneous fluid structure and particle dispersion

Both 2D and 3D simulations reveal the evolution of the turbulent flow, including roll up, growth, merging and breaking up of vortices as shown in Fig. 9-10.

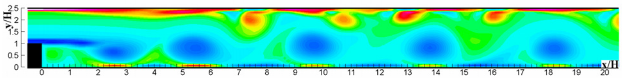

Fig. 9. Vorticity contours of the gas phase (2D)

In 2D simulation, vortices shed behind the step grow up and convect with the main flow in an orderly manner as shown in Fig. 9. However, it is rare to find the breaking up of vortices in 2D simulations.

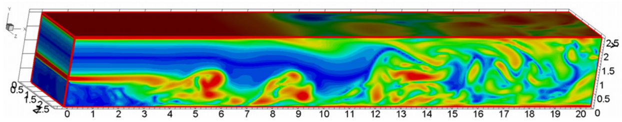

Fig. 10. Vorticity contours of the gas phase (3D)

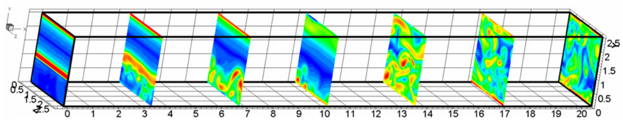

Fig. 11. Sectional view of vorticity contours of the gas phase (3D)

However, the flow becomes more complex in 3D simulation as shown in Fig. 10. The shed vortices break up frequently to smaller ones. Some small vortices deform by stretching and folding. Fig. 11 shows the different sectional views of vorticity contours of the gas phase. The vortical structure is revealed to be essentially three-dimensional, especially downstream.

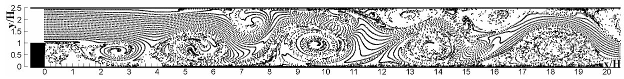

Fig. 12 (a). Particle 2D dispersion (1μm)

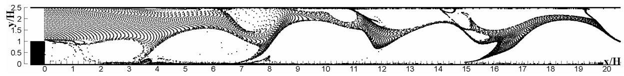

Fig. 12 (b). Particle 2D dispersion (20μm)

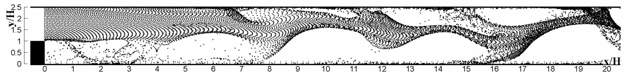

Fig. 12 (c). Particle 2D dispersion (50μm)

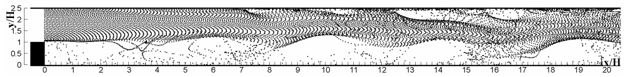

Fig. 12 (d). Particle 2D dispersion (100μm)

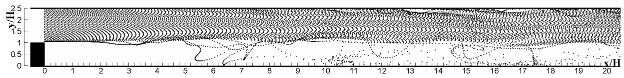

Fig. 12 (e). Particle 2D dispersion (200μm)

The Stokes number used to characterize the motion of selected particle is defined as the ratio of the modified particle dynamic relaxation time $\tau_p$ to the fluid time scale $\tau_f$ in the flow. Where $\tau_p = (\rho_p d_p^2)/(18\mu_f(1+0.15\mathrm{Re}_p^{0.687}))$ and $\tau_f = 5H/U$ [1], based on the approximate large-eddy passing frequency in the separated shear layer. Glass particles of the same size are introduced into the flow when the simulation results of the gas phase become steady. Fig. 12-13 show 2D and 3D particle dispersion with different diameter of 1, 20, 50, 100 and 200μm respectively. The corresponding Stokes numbers are 0.0006, 0.2, 1.06, 3.7 and 11.9.

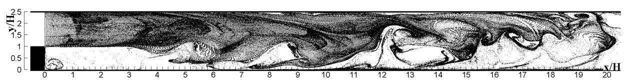

Fig. 13 (a). Particle 3D dispersion (1μm)

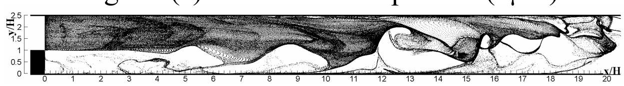

Fig. 13 (b). Particle 3D dispersion (20μm)

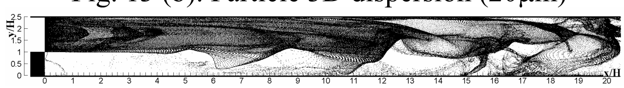

Fig. 13 (c). Particle 3D dispersion (50μm)

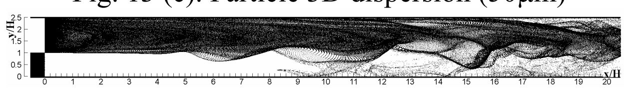

Fig. 13 (d). Particle 3D dispersion (100μm)

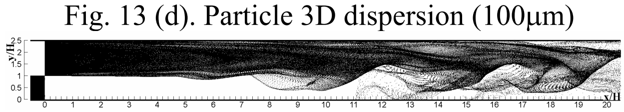

Fig. 13 (e). Particle 3D dispersion (200μm)

Figure 13 shows the particle dispersion in the central *x-y* section. Both 2D and 3D simulation results show similar behaviour of particle dispersion in backward-facing step. Fig. 12(a) and Fig. 13(a) resemble that of the vorticity structure of the gas flow shown in Fig. 9 and Fig. 10 respectively. The relaxation time of these small particles of extreme low Stokes number of 0.0006 is much smaller than the gas time scale so that the particle has sufficient time to respond to the turbulence structure of the fluid flow. Hence the motion of small particles is fully controlled by the vortex structure of the gas phase. Particles in the recirculation zones by 2D prediction are much abundant than those by 3D prediction. The absence of spanwise movement in 2D simulation may increase the probability of such particles to go into the recirculation zone.

As the size of the particles increases, the effect of vorticity on particles becomes less efficient. Fig. 12(b) and Fig. 13(b) show that the 20μm particles have the characteristic of preferential concentration along the boundary of the vortex structure [20]. The decreasing influence of vortex structure on particles of larger Stokes numbers is shown in Fig. 12(c)-(e) and Fig. 13(c)-(e). Most particles of the largest size in Fig. 12(e) and Fig. 13(e) can penetrate through the vortical structure with little transverse dispersion. This is because particles with largest Stokes number have the highest momentum and their motion is least influenced when the gas flow slows down or change direction. The largest particles do not go into the recirculation zone for both 2D and 3D simulation.

## 5 Conclusions

Both 2D and 3D numerical simulations of two-phase turbulent flow over a backward-facing step are successfully investigated by large eddy simulation for the gas phase and a Lagrangian tracing model for the particle phase.

Based on the simulation results, 3D simulation can predict successfully both mean and fluctuating statistical properties. 2D simulation can only reveal the mean statistical properties, but is poor for predicting fluctuating statistical properties. As turbulence is essentially three dimensional, two-dimensional simulation may lose a lot of fluctuating information. 3D simulation is therefore necessary for two-phase turbulent flow.

Predicted instantaneous turbulent flows resulted from 2D and 3D simulations are very much different. The evolutions of vortices are much more regular in 2D simulation that the vortices leave the channel in an orderly manner. The 3D simulated flow is more turbulent, becoming complex and dissimilar as it moves downstream.

Both 2D and 3D simulation give similar results on particle dispersion. For the smallest particles, the ratio of particle relaxation time to the gas integral time scale is much less than 1. These particles are strongly controlled by the vortices structure of the gas phase and follow closely to the gas vortices.

Such particles are not preferentially concentrated. Particles with time scales of similar order as the fluid time scale will be centrifuged out by a vortex and will be preferentially concentrated along the edge of the gas vortices. For large particles, the ratio of particle relaxation time to the gas integral time scale is much great than 1. These particles are more persistent in maintaining their own movement. They do not essentially respond to the vortex motion within the fluid time scale available and will also not be preferentially concentrated.

## 6 Acknowledgements

This work was supported by the Research Grants Council of the Hong Kong Special Administrative Region (Project No. PolyU 5150/02E (B-Q554)).

*Reference:*

[1] Fessler, J.R. and J.K. Eaton, Turbulence modification by particles in a backward-facing step flow, *Journal of Fluid Mechanics*, Vol.394, 1999, pp. 97-117.

[2] Hunt, J.C.R., Industrial and Environmental Fluid-Mechanics, *Annual Review of Fluid Mechanics*, Vol.23, 1991, pp. 1-41.

[3] Sirignano, W.A., Fluid-Dynamics of Sprays - 1992 Freeman Scholar Lecture, *Journal of Fluids Engineering-Transactions of the Asme*, Vol.115, No.3, 1993, pp. 345-378.

[4] Ghosh, S. and J.C.R. Hunt, Induced Air Velocity within Droplet Driven Sprays, *Proceedings of the Royal Society of London Series a-Mathematical Physical and Engineering Sciences*, Vol.444, No.1920, 1994, pp. 105-127.

[5] Armaly, B.F., F. Durst, J.C.F. Pereira, and B. Schonung, Experimental and Theoretical Investigation of Backward-Facing Step Flow, *Journal of Fluid Mechanics*, Vol.127, 1983, pp. 473-496.

[6] Durst, F. and J.C.F. Pereira, Time-Dependent Laminar Backward-Facing Step Flow in a Two-Dimensional Duct, *Journal of Fluids Engineering-Transactions of the ASME*, Vol.110, No.3, 1988, pp. 289-296.

[7] Yu, K.F., K.S. Lau, and C.K. Chan, Numerical simulation of gas-particle flow in a single-side backward-facing step flow, *Journal of Computational and Applied Mathematics*, Vol.163, No.1, 2004, pp. 319-331.

[8] Chan, C.K., H.Q. Zhang, and K.S. Lau, Numerical simulation of gas-particle flows behind a backward-facing step using an improved stochastic separated flow model, *Computational Mechanics*, Vol.27, No.5, 2001, pp. 412-417.

[9] Kaiktsis, L., G.E. Karniadakis, and S.A. Orszag, Onset of 3-Dimensionality, Equilibria, and Early Transition in Flow over a Backward-Facing Step, *Journal of Fluid Mechanics*, Vol.231, 1991, pp. 501-528.

[10] Barton, I.E., Laminar flow over a backward-facing step with a stream of hot particles, *International Journal of Heat and Fluid Flow*, Vol.18, No.4, 1997, pp. 400-410.

[11] Smagorinsky, J., General circulation experiments with primitive equations, *Monthly Weather Review*, Vol.91, 1963, pp. 99-164.

[12] Morinishi, Y., T.S. Lund, O.V. Vasilyev, and P. Moin, Fully conservative higher order finite difference schemes for incompressible flow, *Journal of Computational Physics*, Vol.143, No.1, 1998, pp. 90-124.

[13] Chorin, A.J., Numerical solution of the Navier-Stokes equations, *Mathematics of Computation*, Vol.22, 1968, pp. 745-762.

[14] Orlandi, P., *Fluid flow phenomena : a numerical toolkit*. 2000, The Netherlands: Kluwer.

[15] James, S. and F.A. Jaberi, Large scale simulations of two-dimensional nonpremixed methane jet flames, *Combustion and Flame*, Vol.123, No.4, 2000, pp. 465-487.

[16] Akselvoll, K. and P. Moin, Large-eddy simulation of turbulent confined coannular jets, *Journal of Fluid Mechanics*, Vol.315, 1996, pp. 387-411.

[17] Fan, L.S. and C. Zhu, *Principles of gas-solid flows*. 1996, New York: Cambridge University Press.

[18] Putnam, A., Integrable form of droplet drag coefficient, *American Recorded Society Journal*, Vol.31, 1961, pp. 1467-1468.

[19] Hardalupas, Y., A.M.K.P. Taylor, and J.H. Whitelaw, Particle Dispersion in a Vertical Round Sudden-Expansion Flow, *Philosophical Transactions of the Royal Society of London Series a-Mathematical Physical and Engineering Sciences*, Vol.341, No.1662, 1992, pp. 411-442.

[20] Squires, K.D. and J.K. Eaton, Preferential Concentration of Particles by Turbulence, *Physics of Fluids A-Fluid Dynamics*, Vol.3, No.5, 1991, pp. 1169-1179.